PHILOSOPHICAL TRANSACTIONS B

royalsocietypublishing.org/journal/rstb

Research

Cite this article: Kolchinsky A. 2025 Thermodynamics of Darwinian selection in molecular replicators. *Phil. Trans. R. Soc. B* **380**: 20240436.
https://doi.org/10.1098/rstb.2024.0436

Received: 8 October 2024
Accepted: 5 June 2025

One contribution of 15 to a theme issue 'Origins of life: the possible and the actual'.

Subject Areas:
theoretical biology, biophysics, ecology

Keywords:
thermodynamics, autocatalysis, evolution, origin of life

Author for correspondence:
Artemy Kolchinsky
e-mail: artemyk@gmail.com

Supplementary material is available online at https://doi.org/10.6084/m9.figshare.c.8001346.

THE ROYAL SOCIETY PUBLISHING

Downloaded from https://royalsocietypublishing.org/ on 02 October 2025

Thermodynamics of Darwinian selection in molecular replicators

Artemy Kolchinsky[1,2]

[1]Pompeu Fabra University, 08003 Barcelona, Spain
[2]Universal Biology Institute, The University of Tokyo, Bunkyo-ku, Tokyo 113-0033, Japan

AK, 0000-0002-3518-9208

We consider the relationship between thermodynamics, fitness and Darwinian selection in autocatalytic molecular replicators. We uncover a thermodynamic bound that relates fitness, replication rate and thermodynamic affinity of replication. This bound applies to a broad range of systems, including elementary and non-elementary autocatalytic reactions, polymer-based replicators and certain kinds of autocatalytic sets. In addition, we show that the critical selection coefficient (the minimal fitness difference visible to selection) is bounded by a simple function of the affinity. Our results imply fundamental thermodynamic bounds on selection strength in molecular evolution, complementary to other bounds that arise from finite population sizes and error thresholds. These bounds may be relevant for understanding thermodynamic constraints faced by early replicators at the origin of life. We illustrate our approach on several examples, including a classic model of replicators in a chemostat.

This article is part of the theme issue 'Origins of life: the possible and the actual'.

1. Introduction

Recent work has uncovered fundamental bounds on the thermodynamic costs of various biomolecular processes, including chemical sensing [1–3], copying of polymer-stored information [4–7] and growth and replication [8–15]. These results are derived from general principles of non-equilibrium thermodynamics—such as flux–force relations and fluctuation theorems [16–19]—that relate the dynamical and thermodynamic properties of non-equilibrium processes. Due to their generality, these bounds shed light on universal thermodynamic constraints on lifelike systems, including modern and protobiological organisms, synthetic life and even possible non-terrestrial lifeforms.

One of the most important properties of living systems is that they undergo Darwinian selection. Generally speaking, Darwinian selection refers to a process in which high-fitness replicators reliably outcompete low-fitness replicators. Darwinian selection can be exhibited by chemical systems, such as individual replicating molecules or networks of molecules [20–31]. Synthesizing such systems has been a major focus of research on the origin of life, given that the emergence of Darwinian selection is considered to be a crucial point in the transition from non-living to living matter [24,29,32–34].

Here, we consider the relationship between thermodynamics and Darwinian selection in minimal chemical systems. This relationship may be particularly relevant for understanding thermodynamic constraints on the origin of life [34–36]. We consider a reactor containing autocatalytic replicators that copy themselves either via elementary reactions, or via more complex multi-step mechanisms. We also consider certain types of collectively autocatalytic sets, where replication involves a cycle of cross-catalytic reactions. Our setup includes many types of molecular replicators previously considered in the literature, including self-complementary and complementary templates, polymer-based replicators and autocatalytic small molecules [37–40]. It also encompasses

© 2025 The Author(s). Published by the Royal Society. All rights reserved.

Downloaded from https://royalsocietypublishing.org/ on 02 October 2025

several classic models of molecular replicators, including the chemostat model [21,23] and Eigen's quasispecies model [20].

Each replicator is associated with three quantities. The first is the *affinity* σ of the replication reaction, the thermodynamic driving force of the reaction. The second is the *replication rate* ρ, the number of copies a replicator makes per unit time under actual conditions. Lastly, in §4, we define the *fitness* f of a replicator as the maximum achievable replication rate, reached in the limit of small concentrations. We show that fitness determines a replicator's ability to invade a given population [41] and to survive a high dilution rate. The introduction of an operational definition of fitness for molecular replicators is an important contribution of our work.

In §5, we derive a thermodynamic bound that relates affinity σ, replication rate ρ and fitness f as

$$\sigma \geq -\ln\left(1-\frac{\rho}{f}\right). \tag{1.1}$$

As we discuss below, affinity is a fundamental thermodynamic cost that captures the dissipated Gibbs free energy (entropy production) in a single replication event. Equation (1.1) implies that a minimum affinity is required to sustain a given replication rate, and that this minimum increases as the replication rate approaches its maximum possible value, the fitness. Conversely, equation (1.1) implies that for a given affinity, there is a fundamental limit on how closely the replication rate can approach its maximum value.

We also derive a thermodynamic bound on the strength of Darwinian selection. Observe that a higher fitness replicator is not always able to outcompete a lower fitness one, as this depends on the fitness difference as well as various environmental and demographic factors [42]. Selection strength can be quantified in terms of the smallest fitness difference that can affect evolutionary outcomes in a given population and environment. This is the so-called *critical selection coefficient* s, the 'resolution limit' below which fitness differences are indiscernible.

To use a well-known example, selection strength in finite populations is limited by the stochasticity of sampling, and a fitter mutant will fixate with high probability only when $s \gg 1/N_e$, where N_e is the effective population size [43]. As another example, Eigen's 'error threshold' implies that selection strength is limited by the mutation rate μ, so that a fitter mutant can dominate the population only when $s > \mu$ [20,44].

In §5, we use the inequality (1.1) to derive a thermodynamic bound on the critical selection coefficient. We suppose that selection is sufficiently strong so that a replicator with fitness f is present in the steady state of a flow reactor, while another replicator type with fitness $f' < f$ is driven to extinction. We show that $s = 1 - f'/f$, the selection coefficient between the two replicators, must obey

$$s \geq e^{-\sigma^*}, \tag{1.2}$$

where σ^* is the affinity of the fitter replicator in steady state. This bound on the strength of selection applies even in the case of infinite populations and error-free replicators. It implies that selecting for a relative fitness difference of s must dissipate more than $-\ln s$ of free energy, a quantity that diverges in the limit of vanishing fitness differences, $s \to 0$. We illustrate this result using a classic model of replicators in a chemostat in §7.

In §8, we extend our results to autocatalytic sets, where replication involves a cycle of cross-catalytic reactions. To do so, we first generalize our notion of fitness to autocatalytic sets and then derive generalized versions of the inequalities (1.1) and (1.2). In these generalizations, σ refers to the affinity of the average cross-catalytic reaction in the cycle.

In principle, our results can also be applied to various real-world molecular replicators, suggesting a route for experimental validation. In figure 1, we use published thermodynamic data to illustrate the bound (1.2) on three real-world replicators. The first is a prion at low pH [51], where $\sigma^* \approx 3.5$ (assuming equal concentrations of native and misfolded form) [45]. The second is an RNA molecule that copies itself using a single RNA ligation [39], with $\sigma^* \approx 5$ under *in vivo* conditions [52,53]. The third is a peptide that copies itself using 'native chemical ligation' [40,54], with $\sigma^* \approx 5.9$ at published concentrations [40].

2. Setup

We consider a chemical reactor at constant temperature and pressure. The reactor contains an ideal well-mixed solution of replicators $X, X', \ldots$ and other chemical species $A_1, A_2, \ldots$ that may serve as substrates and side products. We study this system in terms of deterministic concentrations, assuming that molecular counts are sufficiently large so that stochastic fluctuations can be ignored. We use x to indicate the concentration of replicator X and $\vec{a} = (a_1, a_2, \ldots)$ to indicate the concentrations of substrates/side products $(A_1, A_2, \ldots)$.

Each replicator X undergoes a reversible autocatalytic reaction of the form

$$X + \sum_{i=1} \alpha_i A_i \rightleftharpoons X + X + \sum_{i=1} \beta_i A_i, \tag{2.1}$$

where α_i and β_i are stoichiometric coefficients of substrate and side products A_i. A simple example of equation (2.1) is autocatalysis from a single substrate, $X + A \rightleftharpoons X + X$, but many other schemes are also possible. The autocatalytic reaction may be elementary, or it may proceed via multiple steps. Different types of replicators will generally have different stoichiometric coefficients α_i, β_i as well as other thermodynamic and kinetic parameters (discussed below).

Downloaded from https://royalsocietypublishing.org/ on 02 October 2025

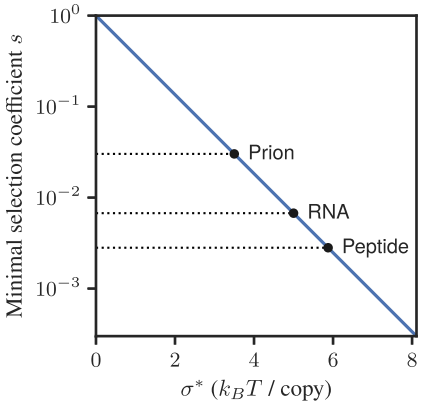

Replicator	Concentrations	$-\Delta G^\circ$
Prion [45]	Equal native and misfolded, pH 3.6	Table 1 [46]
RNA [39]	*In vivo* [47,48]	*In vivo* [47,48]
Peptide [40]	Substrate 90 μM, replicator 5 μM [40]	Figure 4 [49]

Figure 1. Illustration of our thermodynamic bound (1.2) for three real-world molecular replicators: a prion [45], an RNA molecule that copies itself via a single ligation [39] and a peptide that copies itself via 'native chemical ligation' [40,46]. Affinities were computed using equation (2.4) from the concentrations and standard Gibbs energies $-\Delta G^\circ$ listed in the table (at room temperature). Note that there is some debate whether prion replication is first-order, like the replicators considered in this article, or instead involves higher-order cooperative interactions [47–50].

We use $\mathcal{J}$ to indicate the net flux across the autocatalytic reaction in equation (2.1). We define the replication rate ρ of replicator X as the net flux per replicator,

$$\rho := \frac{\mathcal{J}}{x}. \tag{2.2}$$

The replicators may also flow out of the volume with dilution rate $\phi \geq 0$. Accounting for both replication and dilution, the concentration of replicator X changes as

$$\dot{x} = \mathcal{J} - \phi x = (\rho - \phi)x. \tag{2.3}$$

We usually leave dependence on time t implicit in our notation. We will use that in steady state, any non-extinct replicator ($x > 0$) must have $\rho = \phi$, meaning that dilution and replication balance.

In writing equation (2.3), we assume that different replicators do not interact directly by consuming each other as substrates or producing each other as side products, although they may interact indirectly via shared substrates/side products A_i. For simplicity, we also ignore the spontaneous degradation of replicators. However, in the electronic supplementary material, §A, we show that our results still hold in the presence of degradation reactions.

Equation (2.3) also assumes that the rate of spontaneous (i.e. non-autocatalytic) formation of the replicator is negligible. This assumption plays an important role in our analyses below, since replicators that can form spontaneously do not exhibit first-order growth, nor do they go completely extinct in steady-state even at large dilution rates. An interesting direction for future work would extend our analysis to replicators with non-negligible rates of spontaneous formation.

As will be noted below, some of our results hold for closed reactors as well as open reactors that exchange matter with their environment [55]. However, our thermodynamic bound on selection (1.2) applies specifically to a flow reactor in steady state. Different types of flow reactors may be considered. One example is the continuous stirred-tank reactor (CSTR) where the dilution rate and inflow rates are constant, which is often used in chemical [56,57] and biological experiments [58–60], and which can also arise naturally (e.g. in a pond fed by a nutrient-rich stream). To avoid confusion, we note that the CSTR is called a *chemostat* in the biological literature [61,62], although in non-equilibrium thermodynamics, the term *chemostat* sometimes refers instead to an external chemical reservoir [63]. Another possible flow reactor is one where the rates of dilution and inflow can vary as a function of the chemical concentrations. An example is provided by Eigen's quasispecies model, where the dilution rate is adjusted to maintain the total concentration of replicators constant [20].

Our main thermodynamic quantity of interest is the affinity σ of the replication reaction (2.1). A reaction proceeds in the forward direction if and only if the affinity is positive, so affinity can be understood as the driving force of the chemical reaction. Equivalently, the affinity is proportional to the Gibbs energy of reaction, the free energy dissipated in a single reaction event. This dissipated free energy is a fundamental thermodynamic cost that represents lost work potential: a reaction with affinity σ can be coupled to a thermodynamically disfavoured 'uphill' reaction and thereby perform up to σ of chemical work per reaction event.

For an ideal solution, we write the affinity in dimensionless units as

$$\sigma = -\ln x + \sum_{i=1}(\alpha_i - \beta_i)\ln a_i - \Delta G^\circ/RT, \tag{2.4}$$

where R is the gas constant, T is the temperature and $-\Delta G^\circ$ is the standard Gibbs energy (in units of joules per mole),

$$-\Delta G^\circ = RT\Big[\ln x^{\mathrm{eq}} - \sum_{i=1}(\alpha_i - \beta_i)\ln a_i^{\mathrm{eq}}\Big]. \tag{2.5}$$

Here, x^{eq} and a_i^{eq} are equilibrium concentrations of X and A_i, as would be reached if the reactor was closed to exchange of matter and allowed to relax completely. As usual, logarithms of concentrations, as in equations (2.4) and (2.5), should be considered

Downloaded from https://royalsocietypublishing.org/ on 02 October 2025

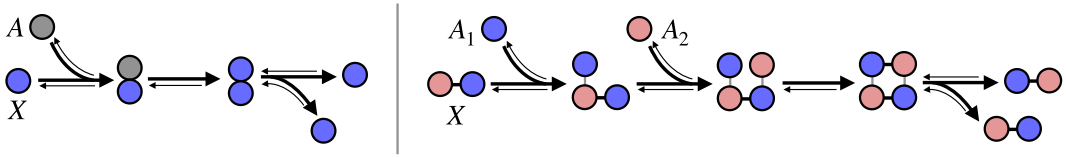

Figure 2. Examples of non-elementary autocatalytic replication mechanisms. *Left*: autocatalysis with binding, conversion and unbinding steps. *Right*: templated replication of a self-complementary polymer (shown here using a dimer).

dimensionless after dividing by the standard concentration (e.g. dividing by $c^\circ = 1\,\mathrm{M}$ if x and a_i are expressed in units of molar concentration).

We emphasize again that we express the affinity σ in dimensionless units. It can be understood in terms of energy units as the number of k_BT dissipated when making a single replicator copy, where k_B is Boltzmann's constant and k_BT is the typical energy (in joules) of a thermal fluctuation at temperature T. In the chemistry literature, σ is often written in units of joules per mole as $-\Delta G = RT\sigma$.

3. Elementary and non-elementary replicators

(a) Elementary replicators

An *elementary replicator* refers to the case where equation (2.1) is an elementary reaction. Then, the net flux across the reaction has the mass-action form [19]

$$\mathcal{J} = rx - r^- x^2, \tag{3.1}$$

with forward and backward rate constants

$$r = \kappa \prod_i a_i^{\alpha_i}, \quad r^- = \kappa e^{\Delta G^\circ/RT} \prod_i a_i^{\beta_i}, \tag{3.2}$$

and κ is a baseline rate constant. Note that r and r^- may depend on the concentrations of substrates/side products $\vec{a}$ (technically, they are 'pseudo rate constants'). We leave this dependence implicit in our notation.

For elementary replicators, the log-ratio of the forward and backward fluxes in equation (3.1) equals the affinity of the replication reaction,

$$\sigma = \ln \frac{rx}{r^- x^2} = \ln \frac{r}{r^- x}, \tag{3.3}$$

as can be verified by comparing equations (3.2) and (2.4). Equation (3.3) is an instance of a general result, called the *flux–force relation* or *local detailed balance* in the literature [64,65], which relates the affinity of an elementary reaction with the forward and reverse fluxes [19]. The flux–force relation is one of the most important results in non-equilibrium thermodynamics, since it connects the kinetic properties of a chemical reaction with its thermodynamic properties.

In fact, our results do not require that the rate constants r and r^- have the mass action form of equation (3.2), only that equations (3.1) and (3.3) hold. In principle, this could be used to study certain non-ideal solutions that exhibit interactions between A_i [66].

(b) Non-elementary replicators

Most real-world autocatalytic replicators cannot be treated as elementary reactions. For this reason, we also consider the case where equation (2.1) represents a reaction mechanism that proceeds via a sequence of m steps,

$$\begin{array}{ccccccc} \sum_i \alpha_{1,i} A_i & & \sum_i \alpha_{2,i} A_i & & \cdots & & \sum_i \alpha_{m,i} A_i \\ X & \rightleftharpoons & Y_1 & \rightleftharpoons & \cdots & \rightleftharpoons & Y_{m-1} \rightleftharpoons X + X. \\ \sum_i \beta_{1,i} A_i & & \sum_i \beta_{2,i} A_i & & \cdots & & \sum_i \beta_{m,i} A_i \end{array} \tag{3.4}$$

Each Y_k is an intermediate chemical species, and each intermediate step is an elementary reversible reaction with mass-action kinetics that may involve substrates/side products A_i with stoichiometric coefficients $\alpha_{k,i}$ and $\beta_{k,i}$. The stoichiometry of the overall reaction is $\alpha_i = \sum_k \alpha_{k,i}$ and $\beta_i = \sum_k \beta_{k,i}$. We assume that intermediate species are not shared between different types of replicators. For simplicity, we also assume that degradation reactions are negligible, although our results generalize to the presence of degradation as shown in the electronic supplementary material, §A.

We term this kind of reaction mechanism a *non-elementary replicator*, although it is also called an 'autocatalytic cycle' in the literature [11,67,68]. A simple example of a non-elementary replicator is a three-step mechanism with binding, conversion and unbinding steps (see figure 2, left). Another example is the step-by-step replication of a self-complementary dimer, illustrated in figure 2 (right), which has been studied in numerous origin-of-life experiments [37,38,69]. Yet other examples include the formose cycle [38] and the autophosphorylation of protein kinase [13,70].

Downloaded from https://royalsocietypublishing.org/ on 02 October 2025

In this subsection, we show that under reasonable assumptions, the production rate and affinity of non-elementary replicators can be expressed in a simple form, somewhat analogous to equations (3.2) and (3.3). Specifically, we will show that the production of a non-elementary replicator can be written in a mass-action-like form,

$$\mathcal{J} = r(\rho)x - r^{-}(\rho)x^2, \tag{3.5}$$

with effective rate constants $r(\rho)$ and $r^{-}(\rho)$ that depend explicitly on the replication rate ρ and implicitly on the dilution rate and the rate constants of intermediate reactions. We will also show that the affinity of a non-elementary replication reaction can be expressed in a 'flux–force-like' form,

$$\sigma = \ln \frac{xr(0)}{x^2 r^{-}(0)} = \ln \frac{r(0)}{xr^{-}(0)}. \tag{3.6}$$

Given equation (3.5), the numerator and denominator can be interpreted as the forward and backward fluxes in the case of $\rho \to 0$, the limit when dilution is much slower than internal reactions. Wachtel *et al*. [64] previously derived this flux–force-like relation for the special case of steady-state conditions.

The rest of this subsection is devoted to the derivation of equations (3.5) and (3.6). Readers not interested in this derivation may skip it without affecting their comprehension of the main message of the article.

Observe that each intermediate reaction $k \in \{1, \dots, m\}$ has net flux

$$J_k = \nu_k y_{k-1} - \nu_k^{-} y_k. \tag{3.7}$$

Here, y_k is the concentration of intermediate species Y_k for $k \in \{1, \dots, m-1\}$, and we use the convention $y_0 = x, y_m = x^2$. The terms ν_k and ν_k^{-} refer to forward and backward (pseudo) rates constants of intermediate steps, typically defined in a manner analogous to equation (3.2). We note that ν_k and ν_k^{-} can depend on the concentrations $\vec{a}$, although we leave this implicit in our notation.

The rate of autocatalytic production of replicator X is

$$\mathcal{J} = 2J_m - J_1, \tag{3.8}$$

since two copies are produced by the last step and one is consumed by the first. The production of intermediate species Y_k ($k \in \{1, \dots, m-1\}$) due to the mechanism is $J_k - J_{k+1}$, since one Y_k is produced by intermediate step k and one is consumed by intermediate step $k+1$. The rate of change of the concentration of the intermediate species, also accounting for dilution with rate $\phi \geq 0$, is

$$\dot{y}_k = J_k - J_{k+1} - \phi y_k. \tag{3.9}$$

To derive equation (3.5), we introduce the assumption that the relative concentrations of intermediate species Y_k and replicator X is approximately constant,

$$\frac{d}{dt}\frac{y_k}{x} = \frac{x\dot{y}_k - \dot{x}y_k}{x^2} \approx 0. \tag{3.10}$$

This assumption always holds in steady state ($\dot{y}_k = \dot{x} = 0$). It also holds under a separation of timescales where relative concentrations y_k/x relax to steady-state values much faster than these steady-state values change (e.g. as a result of changing dilution rate and concentrations $\vec{a}$). This separation of timescales is valid during the exponential growth phase of an initially rare replicator, when the absolute concentrations of x and y_k are small and have a minimal effect on other variables.

Our assumption (3.10) of stationary *relative* concentrations is somewhat different from the quasi-steady-state (QSS) approximation, as often employed in biochemistry [71] and recently considered in non-equilibrium thermodynamics [64,72]. QSS assumes that the *absolute* concentrations of intermediate species y_k are approximately stationary, compared to the rate of change of the replicator concentration x. This assumption can be violated in growing autocatalytic replicators, even if the *relative* concentrations are nearly stationary (e.g. when the intermediate species and replicator grow quickly but at the same rate).

Plugging $\dot{x} = (\rho - \phi)x$ and $\dot{y}_k = J_k - J_{k+1} - \phi y_k$ into equation (3.10) and simplifying gives

$$J_k - J_{k+1} = \rho y_k. \tag{3.11}$$

Using equation (3.7), we express the intermediate concentrations $\vec{y} = (y_1, \dots, y_{m-1})$ in terms of a linear system

$$[(M + \rho I)\vec{y}]_k = \delta_{k,1}\nu_1 x + \delta_{k,m-1}\nu_m^{-} x^2, \tag{3.12}$$

where $M \in \mathbb{R}^{(m-1)\times(m-1)}$ is a matrix of intermediate rate constants,

$$M = \begin{bmatrix} \nu_1^{-} + \nu_2 & -\nu_2^{-} & 0 & 0 & \dots \\ -\nu_2 & \nu_2^{-} + \nu_3 & -\nu_3^{-} & 0 & \dots \\ 0 & \dots & \dots & \dots & -\nu_{m-1}^{-} \\ \dots & 0 & 0 & -\nu_{m-1} & \nu_{m-1}^{-} + \nu_m \end{bmatrix} \tag{3.13}$$

For any $\rho \geq 0$, $M + \rho I$ is an 'M-matrix', so it is invertible and all entries of its inverse are non-negative [73,74].

Downloaded from https://royalsocietypublishing.org/ on 02 October 2025

Finally, we solve equation (3.12) for $\vec{y}$ and combine with equations (3.8) and (3.7) to write the production rate in the form of equation (3.5), $\mathcal{J} = r(\rho)x - r^-(\rho)x^2$. The effective rate constants are

$$\begin{aligned} r(\rho) &:= \nu_1 \left(\nu_1^- G_{11} + 2\nu_m G_{m-1,1} - 1\right) \\ r^-(\rho) &:= \nu_m^- \left(2 - 2\nu_m G_{m-1,m-1} - \nu_1^- G_{1,m-1}\right), \end{aligned} \tag{3.14}$$

where for convenience we defined the matrix

$$G := (M + \rho I)^{-1}. \tag{3.15}$$

These effective rate constants can depend on concentrations $\vec{a}$ (since ν_k and ν_k^- depend on them), although we leave this dependence implicit in our notation.

Below we will use that the first and second derivatives of the effective rate constants obey

$$\begin{aligned} \partial_\rho r(\rho) \le 0, \quad \partial_\rho^2 r(\rho) \ge 0 \\ \partial_\rho r^-(\rho) \ge 0, \quad \partial_\rho^2 r^-(\rho) \le 0. \end{aligned} \tag{3.16}$$

This follows from equation (3.14) by using matrix calculus and the fact that all entries of G are non-negative.

For $\rho = 0$, the effective rate constants can be expressed in closed form,

$$r(0) = \left[\sum_{k=1}^{m} \frac{\prod_{l=1}^{k-1} \nu_l^-}{\prod_{l=1}^{k} \nu_l}\right]^{-1} \qquad r^-(0) = r(0) \prod_{k=1}^{m} \frac{\nu_k^-}{\nu_k} \tag{3.17}$$

as shown in the electronic supplementary material, §B. The $\rho = 0$ regime corresponds to the limit where the replication rate ρ is much slower than the rate of internal reactions, so that ρ can be neglected when solving the linear system (3.12).

The effective reverse rate constant $r^-(\rho)$ is always non-negative, since $r^-(0) \ge 0$ and $\partial_\rho r^-(\rho) \ge 0$ from equations (3.16) and (3.17). On the other hand, formally, the effective forward rate constant $r(\rho)$ becomes negative for sufficiently large ρ, as can be seen from equation (3.14) and $G \to 0$ as $\rho \to \infty$. However, in the following, we only consider the physically meaning range of ρ for which $r(\rho)$ is non-negative, as discussed below in our definition of fitness (4.1).

We finish by discussing the thermodynamics of non-elementary replicators. The affinity of intermediate reaction k in equation (3.4) is

$$\sigma_k = \ln \frac{y_{k-1}}{y_k} + \sum_{i=1} (\alpha_{k,i} - \beta_{k,i}) \ln a_i - \Delta G_k^\circ / RT, \tag{3.18}$$

where $y_0 = x, y_m = x^2$ (as above). Since intermediate reactions are elementary, the forward and backward fluxes in equation (3.7) obey the flux–force relation,

$$\sigma_k = \ln \frac{\nu_k y_{k-1}}{\nu_k^- y_k}, \tag{3.19}$$

as can be shown explicitly when the rate constants ν_k and ν_k^- have mass-action kinetics similar to equation (3.2). The affinity of the overall replication mechanism is the sum of the affinities of the individual steps [19],

$$\sigma = \sum_{k=1}^{m} \sigma_k = \ln \frac{1}{x} + \sum_{k=1}^{m} \ln \frac{\nu_k}{\nu_k^-}. \tag{3.20}$$

We arrive at equation (3.6) by combining equations (3.17) and (3.20).

Observe that an elementary replicator is a special case of a non-elementary replicator with a single reaction ($m = 1$) and no intermediate species. In this case, the effective rate constants in equation (3.14) lose dependence on ρ and reduce to equation (3.17) which in turn reduces to equation (3.2). The mass-action form of equation (3.5) reduces to equation (3.1), and the flux–force relation (3.6) is equivalent to equation (3.3).

4. Fitness and selection coefficient

The concept of *fitness* can be defined differently in different evolutionary scenarios, and finding an appropriate definition is an important area of research in biology and ecology [41,75–77]. Here, we propose a definition of fitness that is suitable for autocatalytic molecular replicators, both elementary and non-elementary.

Before proceeding, we note that one could simply define fitness as the replication rate ρ at a given point in time. However, this definition runs into problems. For instance, for a reactor in steady state, all non-extinct replicators have the same replication rate (the steady-state dilution rate ϕ), while all extinct replicators have an undefined replication rate. This makes it impossible to ask important questions, like whether higher fitness replicators do better than lower fitness ones. At a more general level, the replication rate ρ is a statistic of actual performance. It does not specify how a replicator would perform in a new environment, as usually desired from a fitness measure [41,75–77].

Downloaded from https://royalsocietypublishing.org/ on 02 October 2025

Instead, we define the fitness f of replicator X via the implicit equation,

$$f = r(f) \geq 0, \tag{4.1}$$

where $r(\cdot)$ is the forward rate constant defined in equation (3.14). As we discuss below, this definition of fitness is experimentally measurable and operationally meaningful. For an elementary replicator, $r(\rho)$ does not depend on ρ and f is simply the rate constant of the elementary reaction in equation (3.2). For a non-elementary replicator, f is the non-negative root of the algebraic expression $\alpha - r(\alpha)$. This expression is strictly increasing in α, ranging from $0 - r(0) \leq 0$ to $r(0) - r(r(0)) \geq 0$, as can be deduced from equations (3.17) and (3.16). There is a unique value of $0 \leq f \leq r(0)$ that satisfies equation (4.1) and it can be found quickly using numerical methods, such as bisection.

In operational terms, the fitness f can be understood as the initial growth rate at small concentrations. Imagine a reactor in steady state that does not contain replicator X at time $t < 0$, and suppose that X is introduced at a small concentration $x(0)$ at $t = 0$. Suppose also that X is an elementary replicator or a non-elementary replicator that obeys equation (3.10) (i.e. relative concentrations of intermediates are approximately stationary). Assuming no dilution or degradation, the replicator's concentration will initially grow as

$$\dot{x} = \mathcal{J} = \rho x \approx r(\rho) x,$$

as follows from equations (2.2) and (3.5), while dropping second-order terms in x. This implies $\rho = r(\rho)$, which is uniquely satisfied by $\rho = f$. Thus, the concentration will initially grow as

$$x(t) \approx e^{tf} x(0). \tag{4.2}$$

Moreover, an initially rare mutant with fitness f will increase in concentration if $f > 0$ and decrease toward extinction if $f < 0$. In biology, this type of fitness measure is called *invasion fitness* [41,77–79], and it has been argued to be a particularly general definition of fitness [41,75]. The derivation above also holds for a flow reactor with dilution rate ϕ, in which case it gives $x(t) \approx e^{t(f-\phi)} x(0)$.

In principle, the initial growth rate is experimentally measurable. The initial concentration $x(0)$ should be sufficiently small so that one can neglect the reverse flux (second term in equation (3.5)) and any impact on the steady-state values of $\vec{a}$ and ϕ over the measurement timescale. At the same time, it should be sufficiently large so that stochastic fluctuations can be ignored.

There is also another interpretation of fitness as the *critical dilution rate*, a quantity that plays an important role in chemostat studies [80,81]. Imagine a steady-state flow reactor with concentrations $\vec{a}$ and steady-state dilution rate $\phi > 0$. Suppose that the reactor contains replicator X at steady-state concentration x^*. Using equation (3.5), we can express x^* as

$$x^* = \begin{cases} \frac{r(\phi) - \phi}{r^-(\phi)} & \text{if } r(\phi) > \phi \\ 0 & \text{otherwise} \end{cases}, \tag{4.3}$$

where we used that $\rho = \phi$ in steady state. Now imagine slowly increasing the dilution rate ϕ while maintaining constant $\vec{a}$ (the concentrations of substrates and waste products). The replicator will be pushed to extinction at the critical dilution rate $\hat{\phi}$ where $\hat{\phi} = r(\hat{\phi})$. Given equation (4.1), the critical dilution is equal to the fitness f. The critical dilution rate is experimentally accessible, as long as it is possible to increase the dilution rate while keeping the concentrations $\vec{a}$ constant.

Most simply, our definition of fitness can be considered as the maximum replication rate that can be achieved by the replicator. That is, it is not difficult to show, for instance by using equation (3.5), that $\rho \leq f$ always. Thus, f sets an upper bound on the replication rate. This bound is approached with the limit of low concentrations and/or high dilution rates.

In addition to fitness, we also make use of the notion of the *selection coefficient* from evolutionary biology. The selection coefficient is a normalized measure of relative fitness difference that ranges from 0 (no difference) to 1 (maximum difference). Given two replicators X and X' with fitness values $f \geq f'$, a common definition of the selection coefficient is [82]

$$s := 1 - \frac{f'}{f}. \tag{4.4}$$

We finish by noting two important details. First, the fitness f depends on the concentrations of substrates and side products $\vec{a}$, although this is left implicit in our notation. These concentrations may be considered as the replicator's ecological environment. Second, in real-world experiments, it is often difficult to measure individual concentrations of replicator and intermediate species. Often what is measured is a weighted sum of concentrations,

$$\omega = c_X x + \sum_{i=1}^{m-1} c_i y_i, \tag{4.5}$$

given some non-negative coefficients c_X and c_i. The interpretations of replication rate, fitness and critical dilution rate generalize to this situation. That is, if the replicator and all intermediate species grow at the same rate ρ, then their weighted sum ω will also grow at the same rate. Similarly, if the replicator and all intermediate species vanish at some critical dilution rate $\hat{\phi}$, then ω will also vanish at that dilution rate.

Downloaded from https://royalsocietypublishing.org/ on 02 October 2025

5. Thermodynamic bounds

To derive our thermodynamic bounds, we consider a replicator X with a non-negative growth rate $\rho \geq 0$. Our first bound relates the affinity of replication σ, the fitness f and the replication rate ρ as

$$\sigma \geq -\ln\left(1-\frac{\rho}{f}\right), \tag{5.1}$$

which appeared as inequality (1.1) in the Introduction. For the special case of a flow reactor in steady state, this bound can be written in terms of the steady-state dilution rate $\phi = \rho$ as

$$\sigma^* \geq -\ln\left(1-\frac{\phi}{f}\right), \tag{5.2}$$

where σ^* is affinity of replication under steady-state concentrations.

To derive this bound, we combine equations (2.2) and (3.5) to express the replicator's concentration as $x = (r(\rho)-\rho)/r^-(\rho)$. Plugging into the expression of σ in equation (3.6) gives

$$\sigma = \ln\left(\frac{r(0)}{r^-(0)}\frac{r^-(\rho)}{r(\rho)-\rho}\right). \tag{5.3}$$

Inequality (5.1) is then equivalent to $\frac{r(0)}{r^-(0)}\frac{r^-(\rho)}{r(\rho)-\rho} \geq f/(f-\rho)$ for $0 \leq \rho \leq f$, which in turn is equivalent to the non-negativity of the function

$$h(\rho) := \frac{r(0)}{r^-(0)} r^-(\rho)(f-\rho) - f(r(\rho)-\rho)\,. \tag{5.4}$$

Taking second derivatives and using equation (3.16) shows that $\partial_\rho^2 h(\rho) \leq 0$, so h is concave. Inspection shows that $h(\rho) = 0$ for $\rho = 0$ and $\rho = f$. Therefore, $h(\rho) \geq 0$ over $0 \leq \rho \leq f$, proving the inequality (5.1).

Inequality (5.2) becomes tight for elementary replicators, where the rate constants $r(\rho)$ and $r^-(\rho)$ do not depend on ρ, so $h(\rho) = 0$ for all ρ. More generally, our bound tends to be tighter for 'effectively' elementary replicators with fast internal rates, so that $r(\rho)$ and $r^-(\rho)$ depend weakly on ρ. For general non-elementary replicators, the bound tends to be tighter near $\rho = 0$ and $\rho = f$, corresponding to equilibrium regime and absolutely irreversible regime, respectively.

We also derive a thermodynamic bound on the selection coefficient, which has implications for the strength of Darwinian selection. We consider a flow reactor in steady state with dilution rate ϕ. Suppose that the reactor contains some replicator X with fitness $f > \phi$, and that a second replicator X' with fitness $f' \leq \phi$ is pushed to extinction. Plugging into inequality (5.2) gives

$$\sigma^* \geq -\ln\left(1-\frac{f'}{f}\right) = -\ln s, \tag{5.5}$$

which appeared as inequality (1.2) in §1. This result is illustrated on a model of replicators in a chemostat in §7.

To build intuition regarding the bound (5.5), we may consider two extreme situations. The first is equilibrium steady state, where the replication rate ρ and the affinity σ vanish for all replicators. All replicators are present in positive equilibrium concentrations that do not depend on fitness, reflecting the fact that Darwinian selection is impossible in equilibrium [20,32]. At the other extreme is the irreversible regime, where each replicator copies itself at its maximum possible rate $\rho = f$ and σ diverges. Typically, steady states do not exist in this regime, since any replicator with $f > \phi$ grows without bound and any replicator with $f < \phi$ decays to extinction. In the special case where a single fittest replicator satisfies $f = \phi$, there is a non-zero steady state containing only that replicator [67,83]. To summarize, all replicators coexist in equilibrium ($\sigma = 0$), while only the fitness replicator can possibly exist in steady state in the irreversible regime ($\sigma \to \infty$). Intermediate values of σ interpolate between these two extremes, permitting steady-state coexistence of some but not all replicators.

The inequalities (5.1) and (5.5) are remarkably general, being independent of most details of the chemical system. For instance, they do not depend on the number of coexisting replicators, the substrates/side products involved in replication, whether the replicators copy themselves via elementary or non-elementary reactions, whether the steady state is near or far from equilibrium, etc. They also do not depend on the dynamical mechanism that leads to a particular steady state. For example, they do not depend on whether replicators experience competitive interactions (e.g. different replicators rely on the same substrate) or not (e.g. different replicators do not share substrates but differ in their kinetic parameters).

6. Example: Self-complementary dimer

To illustrate our results on a concrete example, we consider a non-elementary replicator that copies itself via the mechanism

$$X + A \rightleftharpoons XA \overset{B}{\rightleftharpoons} XAB \rightleftharpoons XX \rightleftharpoons X + X$$

X is a self-complementary dimer while A and B are substrates, while the reaction $XAB \rightleftharpoons XX$ is a ligation that produces the bound dimer XX. This type of system was studied in many early experiments on self-replicating chemical systems [69,84–87]. It is shown schematically in figure 2 (right).

Downloaded from https://royalsocietypublishing.org/ on 02 October 2025

We parameterize the rate constants of the two binding reactions, $X + A \rightleftharpoons XA$ and $XA + B \rightleftharpoons XAB$, as

$$\nu_1 = \kappa a \qquad \nu_1^- = \kappa e^{\Delta G_1^\circ/RT}$$
$$\nu_2 = \kappa b \qquad \nu_2^- = \kappa e^{\Delta G_2^\circ/RT},$$

where a and b are concentrations of A and B. The rate constants for ligation $XAB \rightleftharpoons XX$ are parameterized as

$$\nu_3 = 1 \qquad \nu_3^- = e^{\Delta G_3^\circ/RT},$$

and for dimerization $XX \rightleftharpoons X + X$ as

$$\nu_4 = \kappa e^{-\Delta G_4^\circ/RT} \qquad \nu_4^- = \kappa.$$

Where possible, we use parameter values from Rebek's system, one of the first molecules that exhibited self-replication in the lab [84,88]. The binding and unbinding reactions are assumed to be essentially in equilibrium, so we use a fast rate constant $\kappa = 10^9$. The standard Gibbs energies for the binding reactions are $-\Delta G_1^\circ/RT = -\Delta G_2^\circ/RT = \ln 60$ (favouring binding), and for dimerization it is $-\Delta G_4^\circ/RT = -\ln 630$ (favouring the bound dimer) [84]. The ligation step is assumed to be highly irreversible, so we use a large standard Gibbs energy of $-\Delta G_3^\circ/RT = 10$.

Following the experimental setup [88], we consider the weighted sum of concentrations

$$\omega = x + y_{XA} + y_{XAB} + 2y_{XX}, \tag{6.1}$$

which is the total concentration of replicators and intermediates, with the bound dimer counting as two copies.

We first consider a closed reactor ($\phi = 0$) which starts from non-equilibrium initial concentrations of substrates $a(0) = b(0) = 8.2$ mM [84]. We choose $x(0) = 0.1\,\mu$M for the initial replicator concentration. For these parameter values and substrate concentrations, we can use equations (3.14) and (4.1) to compute the fitness as

$$f \approx 0.14.$$

Figure 3a shows the time-dependent concentrations, along with predicted growth at small concentration ($\omega(0)e^{tf}$, dashed line). We see that fitness accurately captures the initial growth rate.

Next, we consider the same system, but now in steady state in a flow reactor. In figure 3b, we show steady-state concentrations across different dilution rates, with substrate concentrations maintained at $a = b = 8.2$ mM. We see that fitness accurately captures the critical dilution rate at which the replicator goes extinct.

Finally, we illustrate our thermodynamic bounds on the same system. Figure 3c shows the affinity of replication versus the bound (5.1) for the system considered in figure 3a, where the replicator grows from a small initial concentration in a closed reactor. The bound is tightest in the regime of low concentrations, achieving an efficiency of $-\ln(1 - \rho/f)/\sigma \approx 0.5$ around $x \approx .1\,\mu$M. In figure 3d, we show the affinity of replication versus our bound (5.2) for the steady-state flow reactor. The bound is tightest near the critical dilution rate, where it achieves an efficiency of $-\ln(1 - \phi/f)/\sigma^* \approx 0.65$.

It should be noted that Rebek's system, like many other self-complementary dimers, is sometimes described as a 'parabolic replicator' with growth obeying a square-root law, $\dot{\omega} \propto \omega^{1/2}$. Square-root growth results because the autocatalyst becomes bound in the thermodynamically favoured dimer XX [88]. In general, however, the type of growth varies with replicator concentration [88]. At low concentrations, the concentration of the dimerized form is small and growth is first order, as seen in the semi-logarithmic plot figure 3a. Square-root growth only appears at larger concentrations, once the concentration of the dimerized form (orange curve in the figure) is sufficiently large.

7. Example: Darwinian selection in a chemostat

We now illustrate our thermodynamic bound on selection using a classic model of autocatalytic replicators in a chemostat (continuous stirred-tank flow reactor) [21].

The reactor may contain up to N replicator types, indicated as $X_1, \ldots, X_N$. Each X_i undergoes an autocatalytic reaction

$$X_i + A \rightleftharpoons X_i + X_i, \tag{7.1}$$

from a shared substrate A. The substrate A is supplied at concentration γ and flow rate ϕ. All species flow out with constant dilution rate ϕ.

For simplicity, we suppose that all replicators copy themselves via elementary autocatalytic reactions. The dynamics of concentrations of replicators x_i and substrate a are

$$\begin{aligned} \dot{x}_i &= k_i x_i \left(a - e^{\Delta G_i^\circ/RT} x_i\right) - \phi x_i \\ \dot{a} &= \phi(\gamma - a) - \sum_i k_i x_i \left(a - e^{\Delta G_i^\circ/RT} x_i\right), \end{aligned} \tag{7.2}$$

where k_i is a rate constant and $-\Delta G_i^\circ/RT$ is the standard Gibbs energy of the reaction (7.1). As usual, we leave dependence on time of $x(t)$ and $a(t)$ implicit.

Although the replicators do not interact directly, they experience an effective interaction due to competition for the shared substrate A. This system is closely related to models of resource competition studied in mathematical ecology and evolutionary

Downloaded from https://royalsocietypublishing.org/ on 02 October 2025

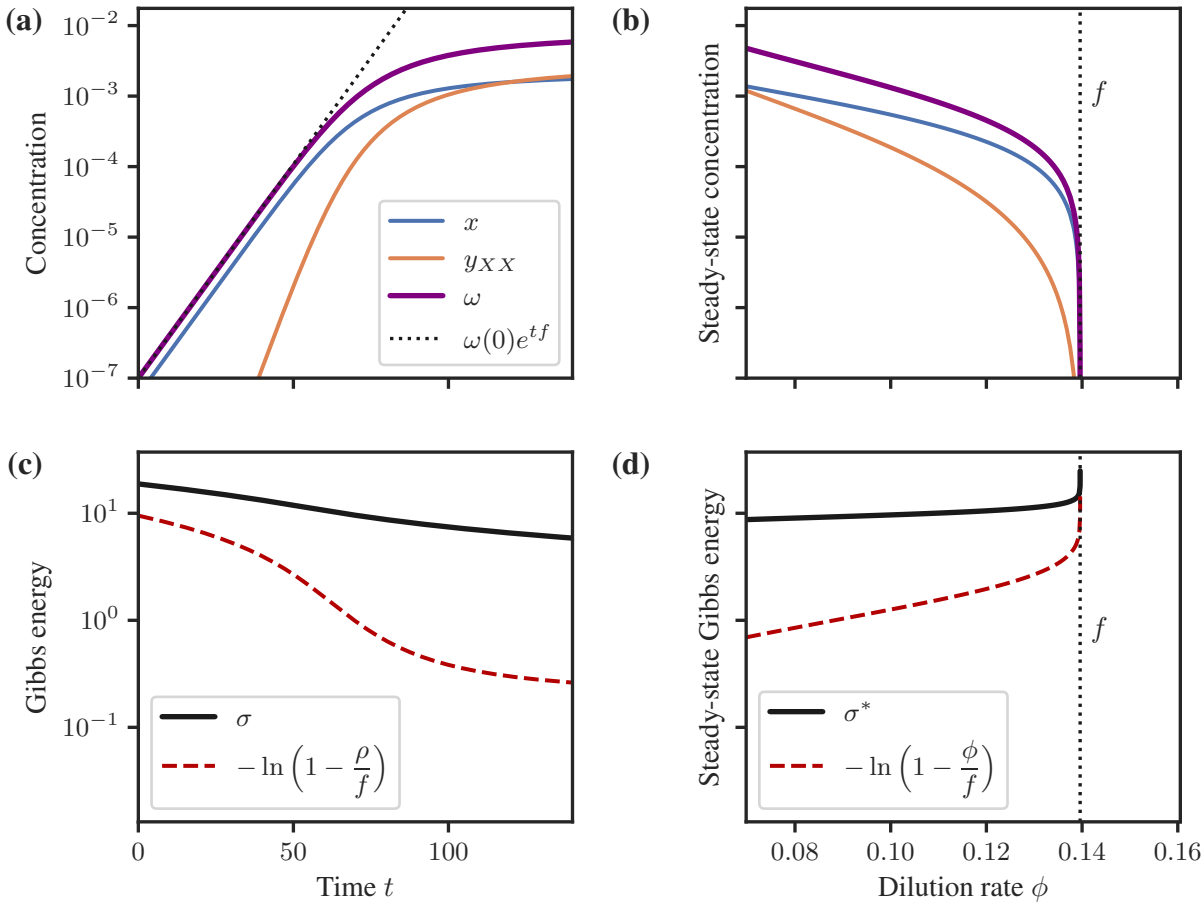

Figure 3. Fitness and thermodynamic bounds illustrated on Rebek's self-complementary dimer [84] with four reactions, as in figure 2 (right). (a) Fitness recovers the initial replication rate given a small starting concentration. We show time-dependent concentrations of replicator x, bound dimer y_{XX}, and weighted sum ω from equation (6.1). (b) Fitness recovers the critical dilution rate in a flow reactor. (c) The bound (5.1) relates replication rate ρ, fitness f and affinity of replication σ. It is shown on the same system as in (a). (d) The bound (5.2) relates fitness, steady-state affinity σ^* and dilution rate ϕ in a steady-state flow reactor. It is shown on the same system as in (b).

biology [58,59,61,62]. Moreover, this system can be mapped onto a competitive Lotka-Volterra system with an effective interaction (see electronic supplementary material, §C).

This type of dynamical system was considered by Schuster and Sigmund [21] (see also [23]). They showed that for any strictly positive initial conditions, there is a unique steady state which governs the long-term behaviour. This steady state is given by a set of coupled equations,

$$a^* = \gamma - \sum_i x_i^*, \quad x_i^* = \max\left\{0, e^{-\Delta G_i^\circ/RT}\left(a^* - \phi/k_i\right)\right\}. \tag{7.3}$$

In the electronic supplementary material, §C, we show how to solve the coupled equations in equation (7.3) by evaluating at most N closed-form expressions.

The strength of selection grows with increasing dilution rate ϕ and/or decreasing substrate feed concentration γ, causing the replicators to be driven to extinction one-by-one in order of increasing k_i. In the electronic supplementary material, §C, we show that replicator X_i becomes extinct once

$$\frac{\gamma}{\phi} \le k_i^{-1} + \sum_{j:k_j \ge k_i} e^{-\Delta G_j^\circ/RT}\left(k_i^{-1} - k_j^{-1}\right). \tag{7.4}$$

Let us consider a concrete example of four replicators with rate constants $(k_1, k_2, k_3, k_4) = (4, 3, 2, 1)$ and $-\Delta G_i^\circ/RT$ values $(1, 2, 3, 2.5)$. Using equation (7.3), we calculate the steady-state concentrations x_i^* of the four replicators at different values of the dilution rate ϕ, while substrate feed concentration is set to $\gamma = 1$. The steady-state concentrations are shown in figure 4 (top). As the dilution rate increases, the replicators go extinct one- by- one in order of increasing k_i. The critical values of ϕ at which each replicator goes extinct, as specified by equation (7.4), are indicated with dotted vertical lines.

In figure 4 (bottom), we show the steady-state affinity of each replicator,

$$\sigma_i^* = \ln\left(a^*/x_i^*\right) - \Delta G_i^\circ/RT. \tag{7.5}$$

The values of σ_i^* grow with increasing ϕ, diverging to infinity as each replicator approaches extinction. We compare σ_1, the affinity of the fittest replicator X_1, to the selection coefficient between X_1 and X_i, $s_i = 1 - f_i/f_1$. Each replicator's fitness is $f_i = k_i a^*$, so $s_i = 1 - k_i/k_1$. As predicted by our bound (5.5), replicator X_i becomes extinct once σ_1^* crosses $-\ln s_i$.

Downloaded from https://royalsocietypublishing.org/ on 02 October 2025

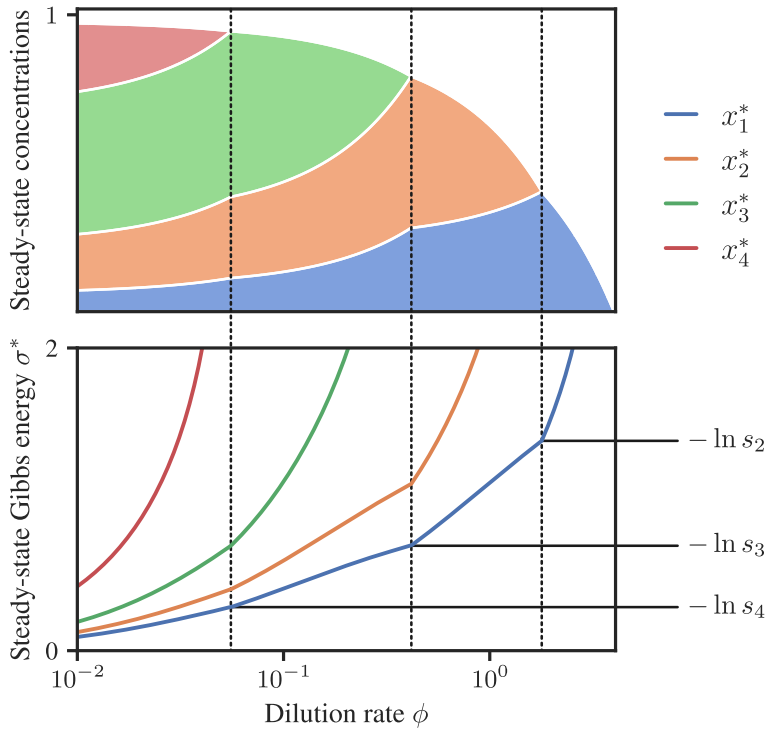

Figure 4. Steady-state behaviour of a system of four elementary replicators, for varying values of the dilution rate ϕ. *Top*: steady-state concentrations of the four replicators. As ϕ increases, the replicators are driven to extinction one- by- one (dashed vertical lines). *Bottom*: as predicted by the bound (5.5), replicator X_i are pushed to extinction once the affinity of the fittest replicator (blue curve) crosses the selection coefficient $-\ln s_i = -\ln(1 - f_i/f_1)$.

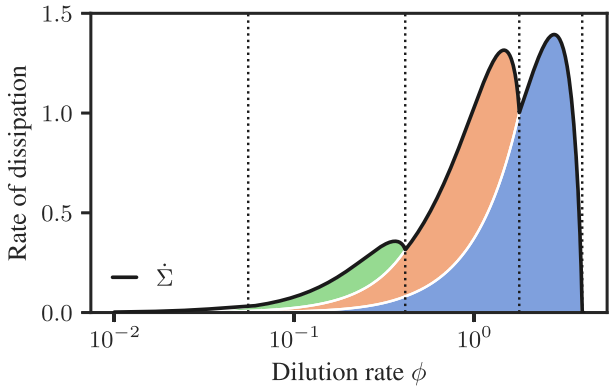

Figure 5. Black curve shows $\dot{\Sigma}$, the overall entropy production rate, equation (7.6), for the four-replicator model as a function of the dilution rate. Shaded regions indicate contributions from different replicator populations, with colours as in figure 4. At the four extinction events (dotted lines), the entropy production rate is continuous but not differentiable, corresponding to second-order non-equilibrium phase transitions.

We note that fitness values do not determine relative concentrations in steady state. For instance, near equilibrium (small dilution rates), steady-state concentrations are determined by the standard Gibbs energies $-\Delta G_i^\circ$ rather than fitness values. This can be seen in figure 4 (top): replicator X_3 has the largest steady-state concentration at small ϕ values, since it has the largest value of $-\Delta G_i^\circ$.

We can also consider the entropy production rate due to replication, i.e. the overall rate of dissipation of Gibbs free energy. In steady state, it is

$$\dot{\Sigma} = \sum_i \jmath_i \sigma_i^* = \phi \sum_i x_i^* \left[\ln\left(a^*/x_i^*\right) - \Delta G_i^\circ/RT\right]. \tag{7.6}$$

Here, we used equation (7.5) and that the steady-state flux across the autocatalytic reaction of replicator X_i is $\jmath_i = \phi x_i^*$.

In figure 5, we plot $\dot{\Sigma}$ for the four-replicator system analysed above. Using shading, we also plot the contribution from each type of replicator, $\phi x_i^* \left[\ln\left(a^*/x_i^*\right) - \Delta G_i^\circ/RT\right]$. As before, we vary the dilution rate ϕ while holding fixed the substrate feed concentration at $\gamma = 1$. Extinction events are marked using vertical dotted lines. Recall from figure 4 that the affinity of replication σ_i^* diverges when replicator X_i approaches extinction. However, the concentration x_i^* vanishes sufficiently fast so that the product $x_i^*\sigma_i^* \to 0$ at extinction. As we show in §C in the electronic supplementary material, $\dot{\Sigma}$ is finite and continuous at the extinction events. Thus, under a common classification scheme [89–93], extinction events are second-order non-equilibrium phase transitions.

Downloaded from https://royalsocietypublishing.org/ on 02 October 2025

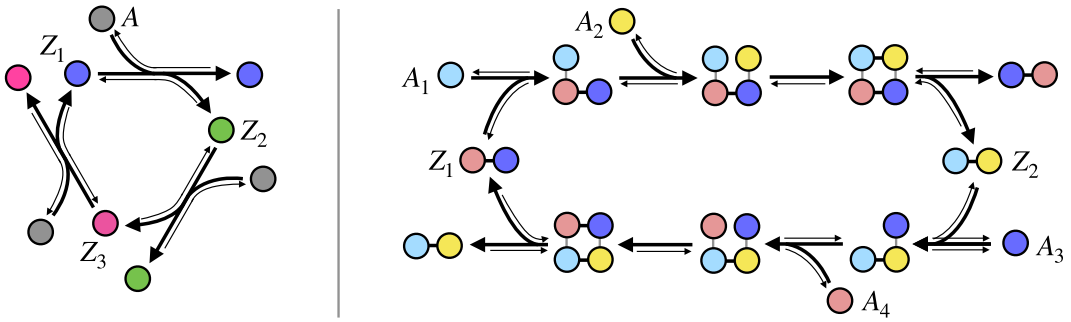

Figure 6. Examples of cross-catalytic cycles. *Left*: a three-element cycle. *Right:* templated replication of complementary polymers (shown here using dimers).

8. Cross-catalytic cycles

We finish by briefly discussing how our results generalize to certain types of autocatalytic sets [94]. For simplicity, we restrict our attention to autocatalytic sets with a uniform and cyclic organization. A general treatment of the thermodynamics of cross-catalytic cycles with arbitrary topologies, kinetics and thermodynamic parameters is an important direction for future work.

We consider an autocatalytic set that contains n species $(Z_1, \dots, Z_n)$ and n reactions, where each species Z_{j-1} catalyses the formation of Z_j:

$$Z_{j-1} + \sum_i \alpha_i^{(j)} A_i \rightleftharpoons Z_{j-1} + Z_j + \sum_i \beta_i^{(j)} A_i. \tag{8.1}$$

The indexes are taken as mod n, so $Z_0 = Z_n$, and $\alpha_i^{(j)}, \beta_i^{(j)}$ indicate stoichiometric coefficients of substrates/side products participating in each reaction. Each catalytic reaction in the cycle may be elementary, or it may be a non-elementary mechanism as in equation (3.4) but with initial reactant X replaced by Z_{j-1} and final products $X + X$ replaced by $Z_{j-1} + Z_j$.

We term this kind of autocatalytic set a *cross-catalytic cycle*. A schematic illustration of a three-member cross-catalytic cycle is shown in figure 6 (left). Cross-catalytic cycles have attracted much attention in work on the origin- of- life, both theoretical [20,95,96] and experimental [26]. An important example of a two-member cross-catalytic cycle is the templated replication of complementary polymers, illustrated in figure 6 (right), which has been investigated in numerous experiments [38,39,97]. In biology, a cross-catalytic cycle called the 'Hinshelwood cycle' has been proposed as a general model of bacterial growth [98,99].

For simplicity, we assume that the cycle is uniform, in the sense that each cross-catalytic reaction has the same kinetic, stoichiometric and thermodynamic properties. Although this assumption seems restrictive, it suffices for studying many autocatalytic sets of fundamental interest, such as complementary pairs with two kinetically and thermodynamically similar cross-catalytic reactions, as in figure 6 (right).

For an autocatalytic set with a uniform cyclic organization, the cycle members Z_j approach equal concentrations $z_j \approx z_k$ after an initial transient. In this regime, we can effectively treat each cycle member Z_j as an independent replicator with autocatalytic flux

$$\mathcal{J}_j = r(\rho) z_j - r^-(\rho) z_j^2. \tag{8.2}$$

Here, $\rho = \mathcal{J}_j / z_j$ is the growth rate and $r(\rho), r^-(\rho)$ are effective forward/backward rate constants, neither of which depend on j due to the assumption of uniformity.

The derivation of equation (8.2) proceeds as follows. When cross-catalytic reactions are elementary, equation (8.2) follows from mass-action kinetics, $\mathcal{J}_j = r z_{j-1} - r^- z_j z_{j-1}$, and the assumption $z_j \approx z_{j-1}$. For non-elementary cross-catalytic reactions with m elementary steps, we consider the different steps that produce or consume Z_j: the m-th step of cross-catalytic reaction j produces one Z_j, the first step of cross-catalytic reaction $j+1$ consumes one Z_j, and the m-th step of cross-catalytic reaction $j+1$ produces one Z_j. The overall production of Z_j due to the cross-catalytic cycle is

$$\mathcal{J}_j = J_m^{(j)} - J_1^{(j+1)} + J_m^{(j+1)}, \tag{8.3}$$

where $J_m^{(j)}$ is the flux across the k-th intermediate step in cross-catalytic reaction j, defined similarly to equation (3.7). Assuming uniformity of kinetics and concentrations, the intermediate fluxes are the same for all j, $J_i^{(j)} = J_i^{(j+1)} \equiv J_i$, therefore

$$\mathcal{J}_j = 2J_m - J_1, \tag{8.4}$$

which recovers equation (3.8). We can then derive equation (8.2) using the same analysis we used for non-elementary replicators in §3b.

Other results follow in a similar manner as for single replicators. For instance, the affinity of each cross-catalytic reaction j is $\sigma_{(j)} = \ln[r(0)/z_j r^-(0)]$, which can be shown using a similar derivation as equation (3.6). The fitness f of replicator Z_j is defined via the relation $f = r(f)$. Using the same approach as in §4, it can be shown from equation (8.2) that this fitness determines both initial growth rate and critical dilution rate.

Combining these results and using the derivation from §5 gives a bound on the affinity of each cross-catalytic reaction j,

$$\sigma_{(j)} \geq -\ln\left(1 - \frac{\rho}{f}\right), \tag{8.5}$$

Downloaded from https://royalsocietypublishing.org/ on 02 October 2025

thereby recovering the analogue of inequality (5.1). In steady state with dilution rate ϕ, this reduces to

$$\sigma^*_{(j)} \geq -\ln\left(1-\frac{\phi}{f}\right), \tag{8.6}$$

where $\sigma^*_{(j)}$ is the affinity of replication under steady-state concentrations.

We may derive a thermodynamic bound on the strength of selection for cross-catalytic cycles, analogous to inequality (5.5). We consider a flow reactor in steady state with dilution rate ϕ that contains a cross-catalytic cycle with fitness $f > \phi$. Suppose there is another replicator X', which may be either a cross-catalytic cycle or an individual autocatalytic reaction, that has fitness $f' \leq \phi$ and is therefore extinct in steady state. Plugging $f' \leq \phi$ into inequality (8.6) gives

$$\sigma^*_{(j)} \geq -\ln\left(1-\frac{f'}{f}\right) = -\ln s. \tag{8.7}$$

This bounds the average affinity of a cross-catalytic reaction in terms of the selection coefficient.

Importantly, these bounds are all stated in terms of the affinity of a single reaction in the cross-catalytic cycle. For example, for a self-replicating complementary polymer as in figure 6 (right), these inequalities bound the affinity of making a single complementary copy, i.e. half of the overall cycle. The combined affinity of all n reactions in the cycle obeys

$$\sum_j \sigma_{(j)} \geq -n\ln\left(1-\frac{\rho}{f}\right). \tag{8.8}$$

Since affinity is equivalent to dissipated Gibbs free energy, equation (8.8) implies that, for a given replication rate and fitness, the thermodynamic dissipation scales linearly with cycle size.

9. Discussion and future work

In this article, we uncovered a general relationship between thermodynamic affinity, fitness and selection strength in molecular replicators. This relationship was derived from the principle of local detailed balance, which plays a central role in non-equilibrium thermodynamics. Our results complement other recent work on fundamental stoichiometric and thermodynamic constraints on autocatalytic replication [14,100–104].

Our approach has similarities to work on competitive exclusion and coexistence theory in microbial ecology [59,62,105]. However, our underlying question differs from the one typically posed in ecology: ecologists aim to explain how diversity is maintained despite competition [105], while we aim to explain how selection (decrease of diversity) occurs despite the drive toward thermodynamic equilibrium. Nonetheless, our work contributes to the study of autocatalytic systems from the perspective of theoretical ecology [22,26–28] and evolutionary theory [24,25,29–31].

Our first inequality (5.1) may be compared to a thermodynamic bound on self-replicating systems derived by England [9]. However, the two bounds make qualitatively different predictions. We refer the reader to Kolchinsky [106] for a critical perspective of the validity of England's bound in application to autocatalytic replicators.

Our thermodynamic bound on selection (1.2) is stated in terms of σ^*, the affinity of replication in steady state. Equation (2.4) implies that the steady-state affinity increases with the standard Gibbs energy $-\Delta G^\circ$ as well as the driving provided by substrates/side products (via the term $\sum_i(\alpha_i - \beta_i)\ln a_i^*$), and that it decreases with the replicator concentration (via the term $-\ln x^*$). Our results do not necessarily imply that selection strength increases with stronger external driving; for instance, it is not always the case that selection becomes stronger if replication is coupled to highly dissipative side reactions. Although increased driving will tend to increase the standard Gibbs energy and the contribution from substrates/side products, it may also decrease the affinity σ by increasing the steady-state replicator concentration x^*. The precise relationship between external driving and σ^* depends on the specifics of the chemical system, and may be an interesting topic to explore in future work. We also note that even if stronger driving does lead to an increase in σ^*, this may not lead to increased selection strength because the inequality (1.2) is not always tight.

We mention some other limitations and directions for future work. First, like many other results derived using local detailed balance, our bound is mostly meaningful for molecular replicators that are not 'too irreversible', meaning that σ is not too large. For instance, the bound (5.1) can be rearranged as $\rho \leq f(1-e^{-\sigma})$, which reduces to the trivial result $\rho \leq f$ once σ is large (e.g. for $\sigma \geq 20$, roughly the dissipation produced by the hydrolysis of a single ATP molecule). Our bound (1.2) on the selection coefficient, $s \geq e^{-\sigma^*}$, also becomes weak for larger σ^*. However, the bound (8.5) for cross-catalytic cycles refers to the affinity of a single reaction in the cycle. It may be applicable to highly dissipative systems that involve large cross-catalytic cycles, as long as the individual reactions in the cycle are not too irreversible.

Another limitation is that we only consider deterministic concentrations, which is justified when molecular counts are large and stochastic fluctuations can be ignored. However, fluctuations cannot be ignored in small systems, nor near extinction events when concentrations approach zero [90,107]. Future work may extend our analysis to the stochastic regime.

Third, we do not consider the effect of mutations. In general, mutations weaken the strength of selection [20]; therefore, we expect that mutations should increase the thermodynamic costs of selection. Future work may verify this prediction and seek stronger bounds on the thermodynamic cost of Darwinian evolution for replicators with mutations. The introduction of mutations leads to other interesting questions concerning the thermodynamic cost of evolution, such as the thermodynamic costs of

finding new high-fitness replicators, rather than merely selecting among existing replicators. In this way, one may investigate the thermodynamics of 'the arrival of the fittest', rather than 'the survival of the fittest' [108,109].

Finally, our study of autocatalytic sets was restricted to the case where reactions are organized in a single uniform cycle. Future work may consider autocatalytic sets with more general topologies, kinetics and thermodynamics [104,110]. Similarly, our analysis of multi-step reaction mechanisms was restricted to linear sequences of reactions such as equation (3.4), which may be generalized in future studies to more complex replication mechanisms.

Ethics. This work did not require ethical approval from a human subject or animal welfare committee.
Data accessibility. Supplementary material is available online [111].
Declaration of AI use. I have not used AI-assisted technologies in creating this article.
Authors' contributions. A.K.: conceptualization, investigation, writing—original draft, writing—review and editing.
Conflict of interest declaration. I declare I have no competing interests.
Funding. This project has received funding from the European Union's Horizon 2020 research and innovation programme under the Marie Skłodowska-Curie Grant agreement no. 101068029.
Acknowledgements. I thank Gülce Kardes, Nathaniel Virgo, Jenny Poulton, David Saakian and Jordi Piñero for useful conversations and suggestions.

Downloaded from https://royalsocietypublishing.org/ on 02 October 2025

References

1. Mehta P, Schwab DJ. 2012 Energetic costs of cellular computation. *Proc. Natl Acad. Sci. USA* **109**, 17978–17982. (doi:10.1073/pnas.1207814109)
2. Barato AC, Hartich D, Seifert U. 2014 Efficiency of cellular information processing. *New J. Phys*. **16**, 103024. (doi:10.1088/1367-2630/16/10/103024)
3. Govern CC, ten Wolde PR. 2014 Energy dissipation and noise correlations in biochemical sensing. *Phys. Rev. Lett*. **113**, 258102. (doi:10.1103/physrevlett.113.258102)
4. Andrieux D, Gaspard P. 2008 Nonequilibrium generation of information in copolymerization processes. *Proc. Natl Acad. Sci. USA* **105**, 9516–9521. (doi:10.1073/pnas.0802049105)
5. Ouldridge TE, R ten Wolde R. 2017 Fundamental costs in the production and destruction of persistent polymer copies. *Phys. Rev. Lett*. **118**, 158103. (doi:10.1103/physrevlett.118.158103)
6. Poulton JM, ten Wolde PR, Ouldridge TE. 2019 Nonequilibrium correlations in minimal dynamical models of polymer copying. *Proc. Natl Acad. Sci. USA* **116**, 1946–1951. (doi:10.1073/pnas.1808775116)
7. Sartori P, Pigolotti S. 2013 Kinetic versus energetic discrimination in biological copying. *Phys. Rev. Lett*. **110**, 188101. (doi:10.1103/physrevlett.110.188101)
8. Kondo Y, Kaneko K. 2011 Growth states of catalytic reaction networks exhibiting energy metabolism. *Phys. Rev. E* **84**, 011927. (doi:10.1103/physreve.84.011927)
9. England JL. 2013 Statistical physics of self-replication. *J. Chem. Phy.* **139**, 121923. (doi:10.1063/1.4818538)
10. Himeoka Y, Kaneko K. 2014 Entropy production of a steady-growth cell with catalytic reactions. *Phys. Rev. E* **90**, 042714. (doi:10.1103/physreve.90.042714)
11. Virgo N, Ikegami T, McGregor S. 2016 Complex autocatalysis in simple chemistries. *Artif. Life* **22**, 138–152. (doi:10.1162/ARTL_a_00195)
12. Saakian DB, Qian H. 2016 Nonlinear stochastic dynamics of complex systems, III: nonequilibrium thermodynamics of self-replication kinetics. *IEEE Trans. Mol. Biol. Multi Scale Commun*. **2**, 40–51. (doi:10.1109/tmbmc.2016.2623598)
13. Bishop LM, Qian H. 2010 Stochastic bistability and bifurcation in a mesoscopic signaling system with autocatalytic kinase. *Biophys. J*. **98**, 1–11. (doi:10.1016/j.bpj.2009.09.055)
14. Piñero J, Solé R. 2018 Nonequilibrium entropic bounds for Darwinian replicators. *Entropy* **20**, 98. (doi:10.3390/e20020098)
15. Corominas-Murtra B. 2019 Thermodynamics of duplication thresholds in synthetic protocell systems. *Life* **9**, 9. (doi:10.3390/life9010009)
16. Beard DA, Qian H. 2007 Relationship between thermodynamic driving force and one-way fluxes in reversible processes. *PLoS One* **2**, e144. (doi:10.1371/journal.pone.0000144)
17. Jarzynski C. 2011 Equalities and inequalities: irreversibility and the second law of thermodynamics at the nanoscale. *Annu. Rev. Condens. Matter Phys*. **2**, 329–351. (doi:10.1146/annurev-conmatphys-062910-140506)
18. Seifert U. 2012 Stochastic thermodynamics, fluctuation theorems and molecular machines. *Rep. Prog. Phys*. **75**, 126001. (doi:10.1088/0034-4885/75/12/126001)
19. Kondepudi D, Prigogine I. 2015 *Modern thermodynamics: from heat engines to dissipative structures*, 2nd edn. Hoboken, NJ: John Wiley & Sons.
20. Eigen M. 1971 Selforganization of matter and the evolution of biological macromolecules. *Naturwissenschaften* **58**, 465–523. (doi:10.1007/BF00623322)
21. Schuster P, Sigmund K. 1985 Dynamics of evolutionary optimization. *Ber. Bunsenges. Phys. Chem.* **89**, 668–682. (doi:10.1002/bbpc.19850890620)
22. Lee DH, Severin K, Ghadiri MR. 1997 Autocatalytic networks: the transition from molecular self-replication to molecular ecosystems. *Curr. Opin. Chem. Biol*. **1**, 491–496. (doi:10.1016/s1367-5931(97)80043-9)
23. Feistel R, Ebeling W. 2011 *Physics of self-organization and evolution*. Weinheim, Germany: Wiley-VCH Verlag GmbH & Co. KGaA. (doi:10.1002/9783527636792)
24. Vasas V, Fernando C, Santos M, Kauffman S, Szathmáry E. 2012 Evolution before genes. *Biol. Direct* **7**, 1. (doi:10.1186/1745-6150-7-1)
25. Takeuchi N, Hogeweg P. 2012 Evolutionary dynamics of RNA-like replicator systems: a bioinformatic approach to the origin of life. *Phys. Life Rev*. **9**, 219–263. (doi:10.1016/j.plrev.2012.06.001)
26. Vaidya N, Manapat ML, Chen IA, Xulvi-Brunet R, Hayden EJ, Lehman N. 2012 Spontaneous network formation among cooperative RNA replicators. *Nature* **491**, 72–77. (doi:10.1038/nature11549)
27. Szilágyi A, Zachar I, Scheuring I, Kun Á, Könnyű B, Czárán T. 2017 Ecology and evolution in the RNA world dynamics and stability of prebiotic replicator systems. *Life* **7**, 48. (doi:10.3390/life7040048)
28. Peng Z, Plum AM, Gagrani P, Baum DA. 2020 An ecological framework for the analysis of prebiotic chemical reaction networks. *J. Theor. Biol*. **507**, 110451. (doi:10.1016/j.jtbi.2020.110451)
29. Ameta S, Matsubara YJ, Chakraborty N, Krishna S, Thutupalli S. 2021 Self-reproduction and Darwinian evolution in autocatalytic chemical reaction systems. *Life* **11**, 308. (doi:10.3390/life11040308)
30. Mizuuchi R, Furubayashi T, Ichihashi N. 2022 Evolutionary transition from a single RNA replicator to a multiple replicator network. *Nat. Commun*. **13**, 1460. (doi:10.1038/s41467-022-29113-x)
31. Ameta S, Arsène S, Foulon S, Saudemont B, Clifton BE, Griffiths AD, Nghe P. 2021 Darwinian properties and their trade-offs in autocatalytic RNA reaction networks. *Nat. Commun*. **12**, 842. (doi:10.1038/s41467-021-21000-1)
32. Bernstein H, Byerly HC, Hopf FA, Michod RA, Vemulapalli GK. 1976 The Darwinian dynamic. *Q. Rev. Biol.* **58**, 186–207.

Downloaded from https://royalsocietypublishing.org/ on 02 October 2025

33. Yarus M. 2011 Getting past the RNA World: the initial Darwinian ancestor. *Cold Spring Harb. Perspect. Biol*. **3**, a003590–a003590. (doi:10.1101/cshperspect.a003590)
34. Jeancolas C, Malaterre C, Nghe P. 2020 Thresholds in origin of life scenarios. *iScience* **23**, 101756. (doi:10.1016/j.isci.2020.101756)
35. Pascal R, Pross A, Sutherland JD. 2013 Towards an evolutionary theory of the origin of life based on kinetics and thermodynamics. *Open Biol*. **3**, 130156. (doi:10.1098/rsob.130156)
36. Danger G, d'Hendecourt LLS, Pascal R. 2020 On the conditions for mimicking natural selection in chemical systems. *Nat. Rev. Chem*. **4**, 102–109. (doi:10.1038/s41570-019-0155-6)
37. Patzke V, von Kiedrowski G. 2007 Self replicating systems. *Arkivoc* **2007**, 293–310. (doi:10.3998/ark.5550190.0008.522)
38. Bissette AJ, Fletcher SP. 2013 Mechanisms of autocatalysis. *Angew. Chem. Int. Ed*. **52**, 12800–12826. (doi:10.1002/anie.201303822)
39. Lincoln TA, Joyce GF. 2009 Self-sustained replication of an RNA enzyme. *Science* **323**, 1229–1232. (doi:%2010.1126/science.1167856)
40. Lee DH, Granja JR, Martinez JA, Severin K, Ghadiri MR. 1996 A self-replicating peptide. *Nature* **382**, 525–528. (doi:10.1038/382525a0)
41. Metz JAJ, Nisbet RM, Geritz SAH. 1992 How should we define 'fitness' for general ecological scenarios? *Trends Ecol. Evol*. **7**, 198–202. (doi:10.1016/0169-5347(92)90073-k)
42. Gillespie JH. 2004 *Population genetics: a concise guide*. Baltimore, MD: Johns Hopkins University Press.
43. Ewens WJ. 2004 *Mathematical population genetics vol. 27: interdisciplinary applied mathematics*. New York, NY: Springer New York. (doi:10.1007/978-0-387-21822-9)
44. Smith JM, Szathmáry E. 1995 *The major transitions in evolution*. Oxford, UK: Oxford University Press.
45. Baskakov IV, Legname G, Prusiner SB, Cohen FE. 2001 Folding of prion protein to its native α-helical conformation is under kinetic control. *J. Biol. Chem*. **276**, 19687–19690. (doi:10.1074/jbc.c100180200)
46. Dawson PE, Muir TW, Clark-Lewis I, Kent SB. 1994 Synthesis of proteins by native chemical ligation. *Science* **266**, 776–779. (doi:10.1126/science.7973629)
47. Eigen M. 1996 Prionics or the kinetic basis of prion diseases. *Biophys. Chem*. **63**, A1–A18. (doi:10.1016/s0301-4622(96)02250-8)
48. Laurent M. 1997 Autocatalytic processes in cooperative mechanisms of prion diseases. *FEBS Lett*. **407**, 1–6. (doi:10.1016/s0014-5793(97)00310-4)
49. Laurent M. 1996 Prion diseases and the 'protein only' hypothesis: a theoretical dynamic study. *Biochem. J*. **318**, 35–39. (doi:10.1042/bj3180035)
50. Femat R, Méndez J. 2011 Mechanisms of prion disease progression: a chemical reaction network approach. *IET Syst. Biol.* **5**, 347–352. (doi:10.1049/iet-syb.2011.0018)
51. Prusiner SB. 1991 Molecular biology of prion diseases. *Science* **252**, 1515–1522. (doi:10.1126/science.1675487)
52. Jülicher F, Bruinsma R. 1998 Motion of RNA polymerase along DNA: a stochastic model. *Biophys. J*. **74**, 1169–1185. (doi:10.1016/s0006-3495(98)77833-6)
53. Erie DA, Yager TD, von Hippel PH. 1992 The single-nucleotide addition cycle in transcription: a biophysical and biochemical perspective. *Annu. Rev. Biophys. Biomol. Struct*. **21**, 379–415. (doi:10.1146/annurev.bb.21.060192.002115)
54. Wang C, Guo Q, Fu Y. 2011 Theoretical analysis of the detailed mechanism of native chemical ligation reactions. *Chem. – Asian J*. **6**, 1241–1251. (doi:10.1002/asia.201000760)
55. Avanzini F, Esposito M. 2022 Thermodynamics of concentration vs flux control in chemical reaction networks. *J. Chem. Phys.* **156**, 014116. (doi:10.1063/5.0076134J)
56. Filisetti A, Graudenzi A, Serra R, Villani M, De Lucrezia D, Füchslin RM, Kauffman SA, Packard N, Poli I. 2011 A stochastic model of the emergence of autocatalytic cycles. *J. Syst. Chem*. **2**, 10. (doi:10.1186/1759-2208-2-2)
57. Semenov SN, Kraft LJ, Ainla A, Zhao M, Baghbanzadeh M, Campbell VE, Kang K, Fox JM, Whitesides GM. 2016 Autocatalytic, bistable, oscillatory networks of biologically relevant organic reactions. *Nature* **537**, 656–660. (doi:10.1038/nature19776)
58. Dykhuizen DE, Hartl DL. 1983 Selection in chemostats. *Microbiol. Rev*. **47**, 150–168. (doi:10.1128/mmbr.47.2.150-168.1983)
59. Grover JP. 1997 *Resource competition*. Boston, MA: Springer US. (doi:10.1007/978-1-4615-6397-6)
60. Hoskisson PA, Hobbs G. 2005 Continuous culture–making a comeback? *Microbiology* **151**, 3153–3159. (doi:10.1099/mic.0.27924-0)
61. Harmand J. 2017 *The chemostat*. Hoboken, NJ: ISTE Ltd/John Wiley, Sons Inc.
62. Smith HL, Waltman PE. 1995 *The theory of the chemostat: dynamics of microbial competition*. Cambridge, UK: Cambridge University Press. (Cambridge Studies in Mathematical Biology 13).
63. Polettini M, Esposito M. 2014 Irreversible thermodynamics of open chemical networks. I. Emergent cycles and broken conservation laws. *J. Chem. Phys*. **141**, 024117. (doi:10.1063/1.4886396)
64. Wachtel A, Rao R, Esposito M. 2018 Thermodynamically consistent coarse graining of biocatalysts beyond Michaelis–Menten. *New J. Phys*. **20**, 042002. (doi:10.1088/1367-2630/aab5c9)
65. Rao R, Esposito M. 2016 Nonequilibrium thermodynamics of chemical reaction networks: wisdom from stochastic thermodynamics. *Phys. Rev. X* **6**, 041064. (doi:10.1103/physrevx.6.041064)
66. Avanzini F, Penocchio E, Falasco G, Esposito M. 2021 Nonequilibrium thermodynamics of non-ideal chemical reaction networks. *J. Chem. Phys*. **154**, 094114. (doi:10.1063/5.0041225)
67. King GaM. 1978 Autocatalysis. *Chem. Soc. Reviews* **7**, 297–316. (doi:10.1039/CS9780700297)
68. Hordijk W. 2017 Autocatalytic confusion clarified. *J. Theor. Biol*. **435**, 22–28. (doi:10.1016/j.jtbi.2017.09.003)
69. von Kiedrowski G. 1986 A self-replicating hexadeoxynucleotide. *Angew. Chem. Int. Ed. Engl*. **25**, 932–935. (doi:10.1002/anie.198609322)
70. Wang ZX, Wu JW. 2002 Autophosphorylation kinetics of protein kinases. *Biochem. J*. **368**, 947–952. (doi:10.1042/bj20020557)
71. Segel LA, Slemrod M. 1989 The quasi-steady-state assumption: a case study in perturbation. *SIAM Review* **31**, 446–477.
72. Avanzini F, Freitas N, Esposito M. 2023 Circuit theory for chemical reaction networks. *Phys. Rev. X* **13**, 021041. (doi:10.1103/physrevx.13.021041)
73. Shivakumar P, Williams JJ, Ye Q, Marinov CA. 1996 On two-sided bounds related to weakly diagonally dominant M-matrices with application to digital circuit dynamics. *SIAM J. Matrix Anal. Appl* **17**, 298–312.
74. Meyer C, Stadelmaier MW. 1978 Singular M-matrices and inverse positivity. *Linear Algebr. Appl.* **22**, 139–156. (doi:10.1016/0024-3795(78)90065-4)
75. Roff DA. 2008 Defining fitness in evolutionary models. *J. Genet*. **87**, 339–348. (doi:10.1007/s12041-008-0056-9)
76. Orr HA. 2009 Fitness and its role in evolutionary genetics. *Nat. Rev. Genet*. **10**, 531–539. (doi:10.1038/nrg2603)
77. Spaak JW, Ke PJ, Letten AD, De Laender F. 2023 Different measures of niche and fitness differences tell different tales. *Oikos* **2023**, e09573. (doi:10.1111/oik.09573)
78. Li Z, Liu B, Li SHJ, King CG, Gitai Z, Wingreen NS. 2020 Modeling microbial metabolic trade-offs in a chemostat. *PLoS Comput. Biol*. **16**, e1008156. (doi:10.1371/journal.pcbi.1008156)
79. Arnoldi J, Barbier M, Kelly R, Barabás G, Jackson AL. 2022 Invasions of ecological communities: hints of impacts in the invader's growth rate. *Methods Ecol. Evol*. **13**, 167–182. (doi:10.1111/2041-210x.13735)
80. Pirt SJ, Kurowski WM. 1970 An extension of the theory of the chemostat with feedback of organisms. Its experimental realization with a yeast culture. *J. Gen. Microbiol*. **63**, 357–366. (doi:10.1099/00221287-63-3-357)
81. Hu WS. 2017 *Engineering principles in biotechnology*. Hoboken, NJ: John Wiley & Sons.
82. Lenski RE, Rose MR, Simpson SC, Tadler SC. 1991 Long-term experimental evolution in *Escherichia coli*. I. Adaptation and divergence during 2,000 generations. *Am. Nat*. **138**, 1315–1341. (doi:10.1086/285289)
83. Lifson S. 1997 On the crucial stages in the origin of animate matter. *J. Mol. Evol*. **44**, 1–8. (doi:10.1007/pl00006115)

84. Tjivikua T, Ballester P, Rebek J. 1990 Self-replicating system. *J. Am. Chem. Soc.* **112**, 1249–1250. (doi:10.1021/ja00159a057)
85. Zielinski WS, Orgel LE. 1987 Autocatalytic synthesis of a tetranucleotide analogue. *Nature* **327**, 346–347. (doi:10.1038/327346a0)
86. Rotello V, Hong JI, Rebek J. 1991 Sigmoidal growth in a self-replicating system. *J. Am. Chem. Soc.* **113**, 9422–9423. (doi:10.1021/ja00024a089)
87. von Kiedrowski G, Wlotzka B, Helbing J, Matzen M, Jordan S. 1991 Parabolic growth of a self-replicating hexadeoxynucleotide bearing a 3′-5′-phosphoamidate linkage. *Angew. Chem. Int. Ed. Engl*. **30**, 423–426. (doi:10.1002/anie.199104231)
88. von Kiedrowski G. 1993 Minimal replicator theory I: parabolic versus exponential growth. In *Bioorganic chemistry frontiers* (eds H Dugas, FP Schmidtchen), pp. 113–146. Berlin, Germany: Springer.
89. Schlögl F. 1972 Chemical reaction models for non-equilibrium phase transitions. *Z. Phys.* **253**, 147–161.
90. McNeil KJ, Walls DF. 1974 Nonequilibrium phase transitions in chemical reactions. *J. Stat.* **10**, 439–448.
91. Zhang Y, Barato AC. 2016 Critical behavior of entropy production and learning rate: Ising model with an oscillating field. *J. Stat. Mech*. **2016**, 113207. (doi:10.1088/1742-5468/2016/11/113207)
92. Tomé T, de Oliveira MJ. 2012 Entropy production in nonequilibrium systems at stationary states. *Phys. Rev. Lett*. **108**, 020601. (doi:10.1103/physrevlett.108.020601)
93. Nguyen B, Seifert U. 2020 Exponential volume dependence of entropy-current fluctuations at first-order phase transitions in chemical reaction networks. *Phys. Rev. E* **102**, 022101. (doi:10.1103/physreve.102.022101)
94. Kauffman SA. 1986 Autocatalytic sets of proteins. *J. Theor. Biol.* **119**, 1–24.
95. Bagley RJ, Farmer JD, Fontana W. 1992 Evolution of a metabolism. *Artif. Life II* **10**, 141–158.
96. Hordijk W. 2019 A history of autocatalytic sets. *Biol. Theory* **14**, 224–246. (doi:10.1007/s13752-019-00330-w)
97. Sievers D, von Kiedrowski G. 1994 Self-replication of complementary nucleotide-based oligomers. *Nature* **369**, 221–224. (doi:10.1038/369221a0)
98. Hinshelwood CN. 1952 On the chemical kinetics of autosynthetic systems. *J. Chem. Soc.* 745–755.
99. Iyer-Biswas S, Crooks GE, Scherer NF, Dinner AR. 2014 Universality in stochastic exponential growth. *Phys. Rev. Lett*. **113**, 028101. (doi:10.1103/physrevlett.113.028101)
100. Despons A, De Decker Y, Lacoste D. 2024 Structural constraints limit the regime of optimal flux in autocatalytic reaction networks. *Communications* **7**, 224. (doi:10.1038/s42005-024-01704-8)
101. Gagrani P, Blanco V, Smith E, Baum E. 2024 Polyhedral geometry and combinatorics of an autocatalytic ecosystem. *J. Math. Chem.* **62**, 1012–1078. (doi:10.1007/s10910-024-01576-x)
102. Marehalli Srinivas SG, Avanzini F, Esposito M. 2024 Characterizing the conditions for indefinite growth in open chemical reaction networks. *Phys. Rev. E* **109**, 064153. (doi:10.1103/PhysRevE.109.064153)
103. Marehalli Srinivas SG, Avanzini F, Esposito M. 2024 Thermodynamics of growth in open chemical reaction networks. *Phys. Rev. Lett*. **132**, 268001. (doi:10.1103/PhysRevLett.132.268001)
104. Blokhuis A, Lacoste D, Nghe P. 2020 Universal motifs and the diversity of autocatalytic systems. *Proc. Natl Acad. Sci. USA* **117**, 25230–25236. (doi:10.1073/pnas.2013527117)
105. Ellner SP, Snyder RE, Adler PB, Hooker G. 2019 An expanded modern coexistence theory for empirical applications. *Ecol. Lett*. **22**, 3–18. (doi:10.1111/ele.13159)
106. Kolchinsky A. 2024 Thermodynamic dissipation does not bound replicator growth and decay rates. *J. Chem. Physics* **161**, 124101. (doi:10.1063/5.0213466)
107. Nitzan A, Ortoleva P, Deutch J, Ross J. 1974 Fluctuations and transitions at chemical instabilities: the analogy to phase transitions. *J. Chem. Phys*. **61**, 1056–1074. (doi:10.1063/1.1681974)
108. Fontana W, Buss LW. 1994 'The arrival of the fittest': toward a theory of biological organization. *Bull. Math. Biol.* **56**, 1–64.
109. Wagner A. 2015 *Arrival of the fittest: how nature innovates*. New York, NY: Penguin Group.
110. Jain S, Krishna S. 1998 Autocatalytic sets and the growth of complexity in an evolutionary model. *Phys. Rev. Lett*. **81**, 5684–5687. (doi:10.1103/physrevlett.81.5684)
111. Kolchinsky A. 2025 Supplementary material from: Thermodynamics of Darwinian selection in molecular replicators. Figshare. (doi:10.6084/m9.figshare.c.8001346)

Downloaded from https://royalsocietypublishing.org/ on 02 October 2025